International Journal of Bifurcation and Chaos

Linking Network Structure and Transient and Equilibrium Integrate-and-Fire Dynamics

Special Issue: Dynamics and Processes on Complex Networks

Cesar H. Comin, João L. B. Batista, Matheus P. Viana, Luciano da F. Costa*
Institute of Physics at São Carlos, University of São Paulo, São Carlos, São Paulo, 13560-970 Brazil

Bruno A. N. Travençolo
Faculdade de Computação, Universidade Federal de Uberlândia, Uberlândia, Minas Gerais, 38400-902 Brazil

Marcus Kaiser
Newcastle University, School of Computing Science, Newcastle upon Tyne, NE1 7RU, United Kingdom

Received (to be inserted by publisher)

The transient and equilibrium properties of dynamics unfolding in complex systems can depend critically on specific topological features of the underlying interconnections. In this work we investigate such a relationship with respect to the integrate-and-fire dynamics emanating from a source node and an extended network model that allows control of the small-world feature as well as the length of the long-range connections. A systematic approach to investigate the local and global correlations between structural and dynamical features of the networks was adopted that involved extensive simulations (one and a half million cases) so as to obtain two-dimensional correlation maps. Smooth, but diverse surfaces of correlation values were obtained in all cases. Regarding the global cases, it has been verified that the onset avalanche time (but not its intensity) can be accurately predicted from the structural features within specific regions of the map (i.e. networks with specific structural properties). The analysis at local level revealed that the dynamical features before the avalanches can be accurately predicted from structural features. Such a prediction is not possible for the dynamical features after the avalanches because the overall topology of the network predominates over the local topology around the source at the asynchronous state.

Keywords: A list of 3–5 keywords are to be supplied.

1. Introduction

Complex networks [Albert & Barabási, 2002; Newman, 2003] have established themselves as a generalized framework for representing, modeling and simulating the most diverse types of discrete dynamical systems involving several interrelated components. Although the initial investigations in this area were mostly

*Corresponding Author: ldfcosta@gmail.com

aimed at structural characterization regarding specific connectivities, especially small-world and scale-free models, the interest of researchers was soon extended to encompass the more general framework about the *relationship between structure and dynamics*. While dynamical systems had often been approached in terms of regular connectivity (e.g. orthogonal or hexagonal grids), the flexibility of complex networks for representing virtually any type of potentially heterogeneous connectivity has paved the way not only for revisiting traditional problems from the perspective of more general connectivities, but also for posing new problems and investigations. The key issue here is that the dynamical properties of a dynamical system underlain by a complex networks is to varying degrees affected or even defined by specific structural features. The identification of how and to which extent structure and dynamics of complex systems affect one another lies at the very heart of scientific modeling.

The present work addresses the relationship between structure and dynamics in networks considering the representative Integrate-and-Fire dynamics [Gerstner & Kistler, 2002]. This model treats the neuronal signals by using a paradigm that needs only to keep track of the spike times of the neurons, which simplifies the overall dynamics and enables to obtain theoretical [Gerstner & Kistler, 2002; Wilson & Cowan, 1972] and simulated [Roxin *et al.*, 2004; Netoff *et al.*, 2004; Kinouchi & Copelli, 2006] results on large systems. More specifically, the network under analysis is understood as a medium with a constant signal source on a fixed node. This signal propagates through the system and its behavior can be measured in two distinct manners, by taking a global or local view of the system (see Figure 1). The global view is the method traditionally used in a range of fields to probe the collective behavior of the system without worrying about the individual signal of the nodes, called a macroscopic view. This approach has the intrinsic advantage of providing theoretical results with methods like mean field or master equation [Barrat *et al.*, 2008; Dorogovtsev & Goltsev, 2008; Boccaletti *et al.*, 2006]. The shortcoming is that much information is lost in the process, and the lost information can only be appropriately recovered through simulations and measurements of the dynamics on individual nodes. Thus, in this work we also take a microscopic view of the dynamics by isolating each possible pairs of nodes as input and output of the dynamics, that is, we ask the following question: for a signal emanating from a source node, what will be the dynamical response in another node of the network? To answer this question we initiate the integrate-and-fire dynamics at a source node s, so that the effect over an output node can be quantified along time. Rodrigues et al. [Rodrigues & Costa, 2009] used this input-output methodology to study signal transmission in cortical networks, finding that it is related to low-pass filtering.

The propagation of integrate-and-fire activation is investigated by considering a combination of two well-known network models, namely the small-world of Watts and Strogatz (WS) [Watts & Strogatz, 1998] and the Waxman (or geographic) [Waxman, 1988] model. This combination, called geographic small-world (GSW) can interpolate between Erdös-Rényi (ER) [Erdős & Rényi, 1960], lattice or geographic networks by tuning two parameters representing the rewiring probability p and spacial constraints α.

It is known [Ahnert *et al.*, 2009] that the presence of a source in the integrate-and-fire dynamic creates avalanches of activation, characterized by the transition between an initial transient phase where there are a small number of spikes occurring at each given time, and an asynchronous state where most of the nodes are spiking. The avalanche arises from the collective behavior of the nodes, and so we use global measurements to characterize the macroscopic properties of the avalanches, with the intent of predicting the time and intensity of them from topological measurements of the source node. We also apply microscopic measurements in order to study the role of the source node on the avalanches. Several interesting results were obtained, including the fact that though the intensity of the avalanches cannot be generally predicted, its onset time can be inferred from topological features.

This article starts by briefly revising the main basic concepts and methods in network construction, the adopted topological measurements and the integrate-and-fire dynamics. It proceeds by presenting the results for a particular network model and the respective interpretation and conclusions.

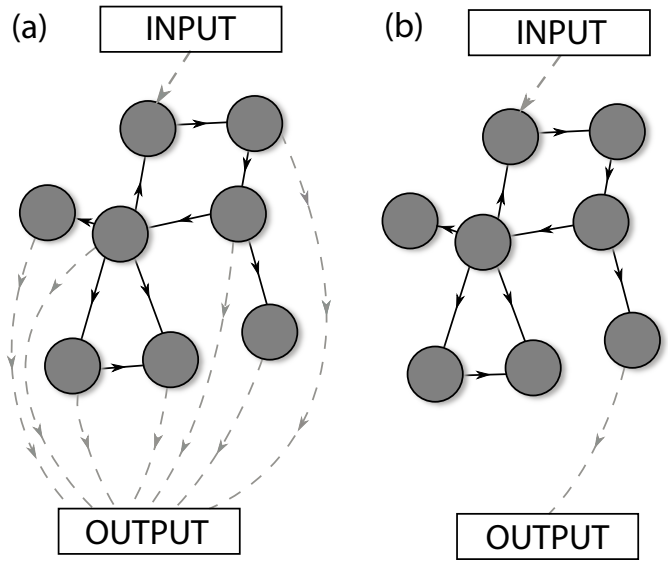

Fig. 1. (a) Global view of the dynamics, where the output reflects the collective behavior of the nodes. (b) Local view, in which we see the network as the medium where the signal of the input node propagates do the output node.

2. Basic Concepts and Methods

2.1. *Complex Networks and Measurements*

A complex network is a graph exhibiting an intricate connectivity. As a graph, it is represented in terms of a set of N nodes and E edges interconnecting those nodes. Each edge extending from node i to node j is denoted as (i,j), with $i, j = 1,2,...,N$ and, in our case, $i \neq j$. The connectivity of a complex network can be fully described in terms of its respective adjacency matrix A, such that the existence of an edge (i,j) implies $A_{ij} = 1$, with $A_{ij} = 0$ being otherwise imposed. In case all edges are reciprocated, the complex network is said to be undirected.

Two nodes are said to be *adjacent* whenever they share an edge, two edges are adjacent if they share a node. The nodes which are directly connected to a given node i correspond to the *immediate neighbors* of i, being called *degree* and represented by the set k_i. A sequence of successively adjacent edges constitute a walk. A walk which never repeats an edge or node is said to be a *path*. The *shortest path* between two nodes is the path which connects those nodes and has the smallest number of edges. The *length* of a walk or path is equal to the respective number of edges. A network is *connected* in case there is at least one path of any length between any of its pairs of nodes.

Given a complex network, it is possible to characterize its connectivity in terms of respective measurements [Costa *et al.*, 2007], such as the node degree and clustering coefficient. These measurements are local, in the sense that they apply to individual nodes, but can be made global by taking their averages through every node of the network.

2.2. *Dynamics: Integrate-and-fire*

Given a network with a specific topology, it can be animated by implementing some specific type of dynamical rules, such as the movement of an agent which chooses with uniform probability each of its next moves. The dynamics implemented in a network can be strongly affected by its respective structure, which constitutes an important subject of current investigation bringing together the areas of complex networks and dynamical systems. In this work we have chosen to investigate the integrate-and-fire dynamics along its transient and equilibrium phases.

The integrate-and-fire dynamic has been widely used in order to model neuronal networks [Gerstner & Kistler, 2002; Ahnert *et al.*, 2009; Guardiola *et al.*, 2000; Rothkegel & Lehnertz, 2009], mainly because it captures the idea of neuronal coding without worrying about the spcifities of the changes in the membrane

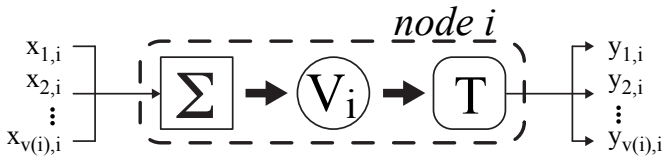

Fig. 2. Node representation for the integrate-and-fire dynamics. The activations enter into a node through the incoming connections x_i and are then summed up by the integrator Σ. The internal state V_i accumulates all the incoming activations. When the value of V_i reaches a given threshold T, the node sends the accumulated activation throughout the outcome links y_i and clear its internal state.

potential (e.g. different post synaptic responses, adaptation, rebound, etc). In this dynamics, the received activations of a particular node are accumulated until it reaches a given threshold. At this stage, the node fires and sends activations (all spikes have intensity 1) through its outgoing neighbors and then return to its resting state. This process can be mathematically expressed as

$$V_i^{t+1} = \begin{cases} V_i^t + \sigma \sum_{j=1}^{N} \sum_f A_{ij} \delta(t - t_j^f) & if\ V_i^t < T \\ \sigma \sum_{j=1}^{N} \sum_f A_{ij} \delta(t - t_j^f) & if\ V_i^t \geq T \end{cases} \quad (1)$$

where V_i^t is the state of node i at time t, t_j^f is the time of the $f-th$ spike of node j and σ the coupling strength (we assume $\sigma = 1$ through this work).

This process is better described by considering a node as the union of five elements, as illustrated in Figure 2: (i) the incoming connections; (ii) the outgoing connections; (iii) the integrator Σ; (iv) the internal state of the accumulated activations V_i; (v) and the threshold T. The role of the incoming connections is to receive the activations coming from one or more neighbors of the node. These activations are them summed up by the integrator Σ, which also updates the internal state V_i by adding the incoming activations. If the level of V_i reaches T, then the node sends activations throughout all of its outgoing edges. This whole process is initiated by the activations originated from the *source nodes*, i.e. those that are continuously firing. We denote by $S_i(t)$ the state of firing of node i, i.e. in the case a spike is taking place at time t then $S_i(t) = 1$, and $S_i(t) = 0$ otherwise. When working with this dynamics it is common to account for the global spike rate of the network along time, defined as

$$R(t) = \frac{1}{N} \sum_{i=1}^{N} S_i(t). \quad (2)$$

3. Experimental Framework

3.1. *Network model used*

In order to better investigate the influence of the topology on the integrate-and-fire dynamic, we introduce the GSW network model (geographical small-world) that can be used to interpolate between a regular lattice and an ER network, while taking into account the distance betweens nodes. Starting with a lattice embedded in a unitary square with aperiodic boundary condition, every edge is rewired with probability p, so that, for one of its ends, another node is chosen in the network with probability $P(\alpha, d_{i,j})$ given by

$$P(\alpha, d_{i,j}) = exp\left[-\frac{\alpha}{1-\alpha} \frac{d_{i,j} - 1/\sqrt{N}}{\sqrt{2} - d_{i,j}} \right] \quad (3)$$

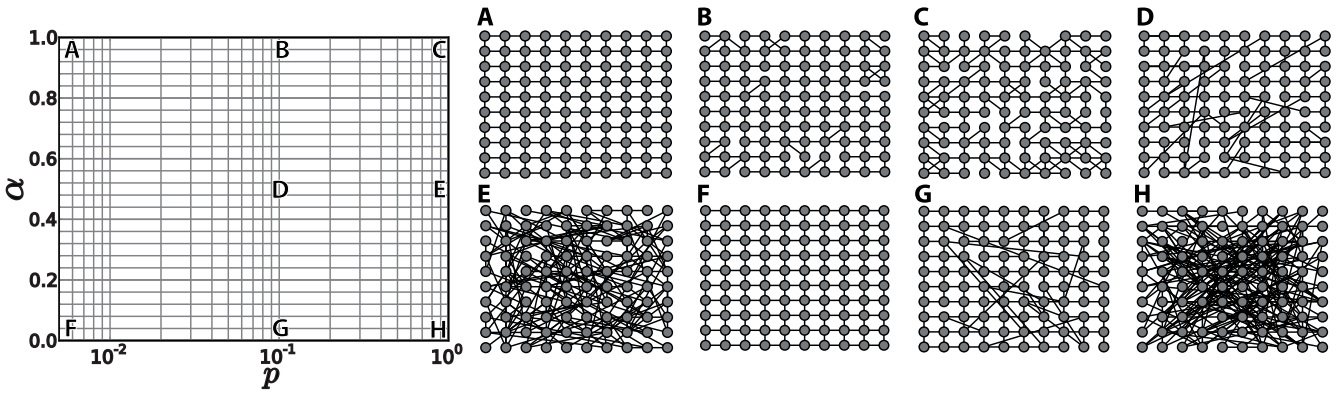

Fig. 3. Examples of networks obtained for the model used in the present work. (left) Bi-dimensional parameter space of α and p. (right) Diversity of topologies that can be produced by the purposed GWS model.

where $d_{i,j}$ is the Euclidean distance between nodes i and j and $\alpha \in [0, 1)$ is a parameter setting how strong is the influence of the medium on the connections. As shown in Figure 3, for $\alpha = 0$ the distance in the embedding space is not taken into account, and setting $p = 0.1$ the shortcuts created induce the well known small world effect characterized by short distances. For $p \to 1$ the structure obtained is almost an ER network. When we set $\alpha \neq 0$ the shortcuts are restricted to regions not far away from the original node and the small world effect tends to be less pronounced. It is important to note that for $\alpha \to 1$ and $p = 0$ the network is still a lattice. Moreover, because the proposed model is based on a rewiring process in a square lattice, the average degree is restricted to 4. We also note that the generated network is not guaranteed to be connected, but the largest component is usually composed by more than 99 percent of the nodes. A similar network model was proposed in [Sen *et al.*, 2002] as a extension of the WS model and embedded in higher dimensions.

3.2. *Network dynamical and structural measurements*

In this paper, we investigate the relationship between the network structure and dynamics by considering several topological and dynamical properties. In this section we describe the parameters used to simulate the integrate-and-fire dynamic over the considered network model, as well as the derived measurements used to characterize this dynamic. In addition, several structural measurements are presented and used to describe the topological properties of the networks. In order to generate the avalanches we begin with all the nodes of the network set to zero potential and randomly choose one source node that generates a spike at each iteration of the dynamics. In order to guarantee that the dynamic will reach an asynchronous state we set the threshold of the neuronal unit to be lower than the mean degree of our network. So, through the remainder of this work we set $T = 3$, unless otherwise noted.

The structural measurements are divided in two groups, one tries to characterize the source by using measurements that probe the entire network structure from the point of view of a single node, which are called global measurements. The other approach uses pairwise measurements in order to quantify the correlation between two given nodes, in the hope to simplify the intricacies of the network structure comprised between them, we call such values local (or pairwise) measurements.

The local structural measurement used is the shortest path length (SPL), defined for two given nodes as the length of the smallest path between them. The specific shortest path between nodes i and j is denoted as SPL_{ij}. The global structural measurements are the average shortest path lengths of the source (SPL_s), defined as

$$SPL_i = \frac{1}{N-1} \sum_{j \neq i} SPL_{ij}. \tag{4}$$

The other global measurement used is the eigenvector centrality (EC), defined for a node i as the i-th

element of the eigenvector associated with the largest eigenvalue of the adjacency matrix of a network. EC_s denotes the EC of the source.

The dynamical measurements we use are also divided in global and local. Traditionally, global measurements are particularly important when one wants to use a single value to characterize the system. Unfortunately, the microscopic information of individual nodes is lost in the process, because there could be groups of nodes following very distinct dynamics which could be not reflected by the global measurement. In order to account for this problem, we also use individual dynamic information that, when combined with pairwise structural information can effectively measure if different nodes feel the dynamic in a different manner. Also, because the dynamics can be either in the transient or asynchronous states (refer do Figure 4), each measurement should be defined for both these states.

Local dynamical measurements are the spike rate before ($R^{(1)}$) and after ($R^{(2)}$) the avalanche onset, defined by

$$R_i^{(1)} = \frac{1}{\tau}\sum_{t=0}^{\tau} S_i(t) \tag{5}$$

$$R_i^{(2)} = \frac{1}{T_s - \tau}\sum_{t=\tau}^{T_s} S_i(t) \tag{6}$$

where T_s is the total time of the simulation, and τ is the instant of the transition between phases 1 and 2. Other considered measurements are the time of first spike of the node (FS), and the inter-spike entropy after τ (ISE), defined by

$$ISE_i = \sum_{\Delta} P(\Delta) log(P(\Delta)) \tag{7}$$

where $P(\Delta)$ is the probability of finding an interval of size Δ between subsequent spikes of node i. The global dynamical measurements that we considered in this paper are the transition time (τ) and the intensity of the avalanche (I_τ), defined as the maximum of the derivative of $R(t)$ (see Figure 4). Finally, to quantify the dispersion of the measurements we use the coefficient of variation (CV) of a variable x, defined as

$$CV(x) = \frac{\sigma(x)}{\mu(x)}. \tag{8}$$

For each pair (α, p) we generate M networks with N nodes using the GSW model defined above. In addition, for each network we randomly choose, with uniform probability, a node as the source. Then we simulate one realization of the integrate-and-fire dynamics for a sufficiently large number of iterations for each network. So we have as result M and $M * N$ sets of global and local measurements, respectively. To quantify how the structure is influencing the dynamic we use the Pearson correlation coefficient that provides a value in the range -1 to 1 for each (α, p). By repeating the process for various (α, p) we can construct a map quantifying the influence of the structure on the dynamics for different topologies (lattice, random and spatially constrained). During the experiments we noted many different behaviors of the system for large α, while small α did not imply such variability. So, we adopt a rescaled version of α, called $\hat{\alpha}$, defined by

$$\hat{\alpha} = \frac{e^{\alpha} - 1}{e - 1}. \tag{9}$$

We recall that the Pearson coefficient quantifies linear dependence between two variables. So, it is possible to check for more general relationships if we take the logarithm of both measurements that are being correlated. For the rest of this work we take the logarithm of the measurements before correlation.

4. Results and discussion

Figure 4 shows an example of a spikegram and the evolution of the spike rate, R along time. In this curve, a period of fast growth is followed by an asynchronous state, where R remains approximately constant. The instant τ when the avalanche occurs can be automatically detected by analyzing the maximum of the derivative of R filtered by a Gaussian function in order to eliminate high frequency noise. Therefore, we split the time evolution of the simulation into two phases: *phase 1* (transient), representing the time interval between the beginning of the simulation until the time of the transition τ; and, *phase 2* (asynchronous) corresponding to the remainder interval from τ to T_s.

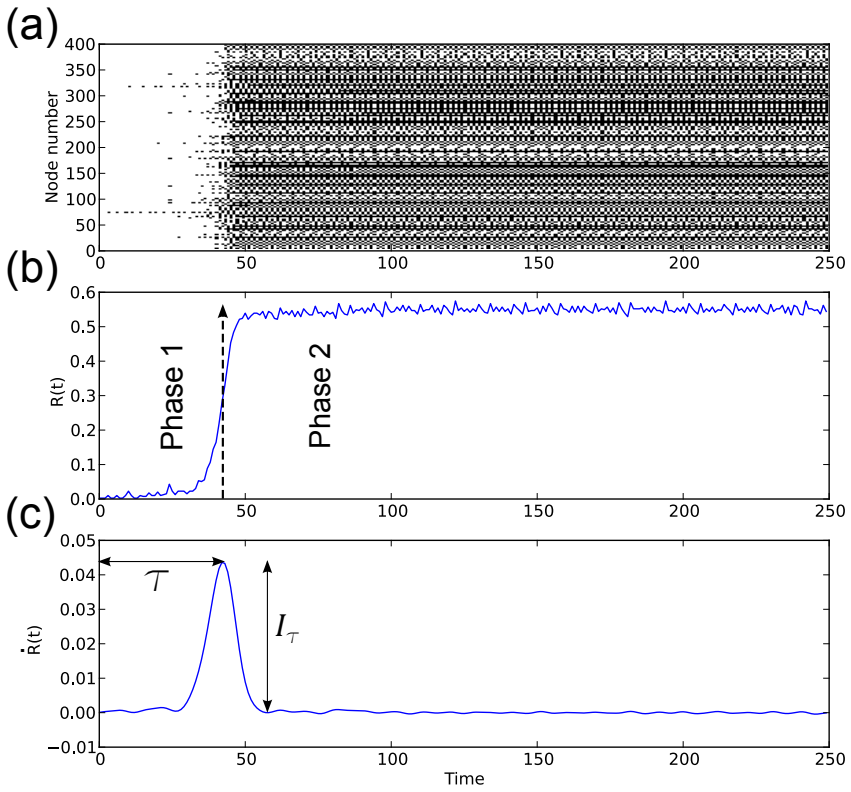

Fig. 4. (a) Example of spikegram, i.e., the state of each node of the network along the simulation, where black dots indicate a spike. (b) The global spike rate ($R(t)$). (c) Global spike rate derivative ($\dot{R}(t)$). Note a clear separation between the transient (phase 1) and the asynchronous (phase 2) of the dynamics. The graphs were obtained for the GSW model with 400 nodes, $p = 1$ and $\alpha = 0.1$.

In order to illustrate how the parameters of the GSW model can affect the behavior of the integrate-and-fire dynamics, in Figure 5 we show the spike rate, R, as a function of time and its derivatives ($\dot{R}$), for different pairs (α, p). It is clear that the avalanches can have very distinct behavior for different topologies. For small p the lattice structure generates a very slow signal propagation and the avalanche is almost undefined. For large p and small α, $R(t)$ has a pronounced transition that divides the dynamic between phases 1 and 2. For large α, the absence of global shortcuts tends to attenuate the transition between states, as we can see in 5(c) and 5(d).

So as to better understand the characteristics of our model and the behavior of the avalanches, in

Figure 6 we show a map of some topological and dynamical measurements averaged for the entire network. For each $(\hat{\alpha}, p)$ we used $M = 1000$ networks with $N = 400$ nodes. Figures 6(a), 6(b) and 6(c) shows the average values of τ (a), I_τ (b), and SPL (c). When we increase p the shortcuts created tends to significantly decrease the $< SPL_s >$, creating a network where the source can efficiently communicate with the rest of the nodes through small paths. As a consequence, τ decreases when p increases. To see why I_τ increases, we remember that for an ER network with $N \to \infty$, the number of nodes at distance h from the source grows exponentially with h [Newman, 2010]. In our case the finite size of the network bounds this growth. For a lattice this number grows linearly in h, until we reach the border, this is a consequence of the different SPL_s between the two models. A more interesting result is the dependence of the measurements with α, although the explanation is the same, as smaller α implies larger $< SPL_s >$, we now have two different behaviors. For small α the system is insensitive to changes in α, but as α increases we observe the emergence of a strong dependence between the system and this parameter. A possible explanation is that different sizes of global shortcuts do not change the system, but when α is large, a transition occurs and the network starts to rapidly loose its global communication.

The result in Figure 6(d), related to the eigenvector centrality, shows a distinct behavior when compared with 6(a), 6(b) and 6(c). To interpret this behavior we first note that the adopted EC values are normalized so as that $max\{EC\} = 1$, and so we can relate $\langle EC \rangle$ with a measurement called Central Point Dominance (CPD) [Costa *et al.*, 2007], given by

$$CPD = \frac{1}{Q} \sum_{i=1}^{N} max\{EC\} - EC_i \tag{10}$$

where Q is a normalization factor. CPD measures how heterogeneous the distribution of centralities is, $CPD = 0$ for a complete graph and $CPD = 1$ for a star graph. It is also clear that

$$CPD \approx \frac{N}{Q} \left(max\{EC\} - \langle EC \rangle \right)$$

$$CPD \propto 1 - \langle EC \rangle \tag{11}$$

which means that as $\langle EC \rangle$ decreases, the distribution of EC gets more heterogeneous. Returning to Figure 6(d), when p is small, equation 11 implies that there are no dominant nodes in the network, every node has approximately the same centrality, which is expected since the topology is still almost a lattice. When we increase p the topology becomes more heterogeneous, and some fairly good connected nodes appears, lowering the mean centrality. A curious result corresponds to the very small values obtained for large p and α - right top corner. It means that in the strongly constrained regime, the centrality values become more heterogeneous than on an ER network. Actually, we observe that the distribution of eigenvector centrality in this region follows a power-law behavior, which is a sound result, given that the degree distribution is a binomial distribution. Figure 7 shows the CV defined in 8 for the four measurements considered, in Figures 7(a) and (b) there is a general rule that lattice-like structures have the larger fluctuations, since for this configuration the avalanches are not well defined and the measurements are prone to errors. We also note the confirmation of the high variability of $\langle EC \rangle$ for large p and α, as shown in Figure 7(d).

In Figure 8 we start to quantitatively study the correlation between structure and dynamic by plotting maps of the Pearson correlation coefficient between structural and dynamical global measurements. Figure 8(a) shows that SPL_s and τ have a very strong correlation for a large range of p and α values. Only for small values of p this correlation becomes less intense. This statement is explained by the already observed large fluctuations for lattice-like structures. In Figure 8(b) the correlation between EC_s and τ share the same behavior of Figure 8(a) with two main differences: first, the relationship is inverse, meaning that when we have a source node with large EC_s, the avalanches take less time to occur. The second difference is that for large p and α the correlation is weak, which indicates that although the centrality of the source

has a strong variability at this regime, given its power law distribution, the times of the avalanches do not follow this variation.

An interesting behavior can be seen in Figure 8(c). For intermediate value of α, the correlations between SPL_s and I_τ increase when p decreases, i.e. when the number of shortcuts in the network decreases. This happens until the number of shortcuts gets very small. That is so because in a lattice, the nodes located near shortcuts (lower SPL) have a natural advantage to spread their signals than nodes that are further away. We can relate this with an epidemic spreading through a large number of countries: the regions near to the airports are the first to get infected [D. Balcan, 2009]. Looking at Figure 8(d) we observe the absence of significant correlations between $\langle EC \rangle$ and I_τ, meaning that $\langle EC \rangle$ may not capture the information about few shortcuts like the SPL. Overall, these results show that, thanks to the high correlations found between the studied variables, for most values of α and p it is easy to predict the time of avalanches if we know the SPL or EC of the source. On the other hand, it is much more difficult to predict the intensity of avalanches.

We now proceed to investigate the dynamics from another point of view. As said before, we can assume the source as providing an input signal, and each other node as an output. Figure 9 shows the correlation between the pairwise measurements. In Figure 9(a) the correlation is negative, this means that when the source is closer to a given node, its spike rate before the transition is larger than that observed for a distant node. Although this result is trivial, it is a good demonstration of the difference between looking at global, as in figure 8, and local measurements. The latter gives us a microscopic view of the dynamics and helps us to understand the mechanisms behind the collective behavior of the nodes. Figures 9(b) and 9(d) show that there is little correlation between the distance from the source and $R^{(2)}$ or ISE, which means that the collective behavior of the nodes is stronger than the local interactions measured, so after the transition, the position of the source no longer plays an important role. In Figure 9(c) we observe a very strong correlation between SPL and FS for all $(\hat{\alpha}, p)$. It is important to note that for large α the role that the space plays on the structure of the network reflects strongly on the dynamics itself, because the wavefront of the signal from the source appears to be more defined, bearing a particularly strong relationship between the first spike of the node and its distance from the source.

5. Conclusion

Complex systems are characterized by diversified dynamics underlain by non-trivial interconnectivity. One of the challenges in understanding such systems is to figure out how the dynamics is influenced or even affected by the topology. The present work addresses this key paradigm with respect to the non-linear integrate-and-fire dynamics and a novel network model that can interpolate between well-known topologies, namely Watts-Strogatz, Erdös-Rényi and lattice. We obtained correlations maps of global and local measurements in order to probe the macro and microscopic behavior of the dynamics. The global maps revealed large fluctuations on regions related to lattice-like structures, which means that in this regime the topology of the source is unimportant when trying to characterize the avalanches. The intensity of the avalanches also turned out to be very hard to predict from the structure only. Still, the time for the avalanches onset showed significant correlations with structural features for a large number of network configurations. We also found that for large p and α our model exhibited a unexpected power-law behavior for the distribution of eigenvector centralities. The maps related to local measurements showed that before the avalanche the local topology of the source plays an essential role on the dynamics of the majority of the nodes, but after the avalanche, a sharp transition unfolds and the collective behavior of the network then overshadows any influence of the source. As a future work, it would be particularly interesting to extend the investigation reported here to the study other real-world systems, such as epidemic or fads spreading in social networks.

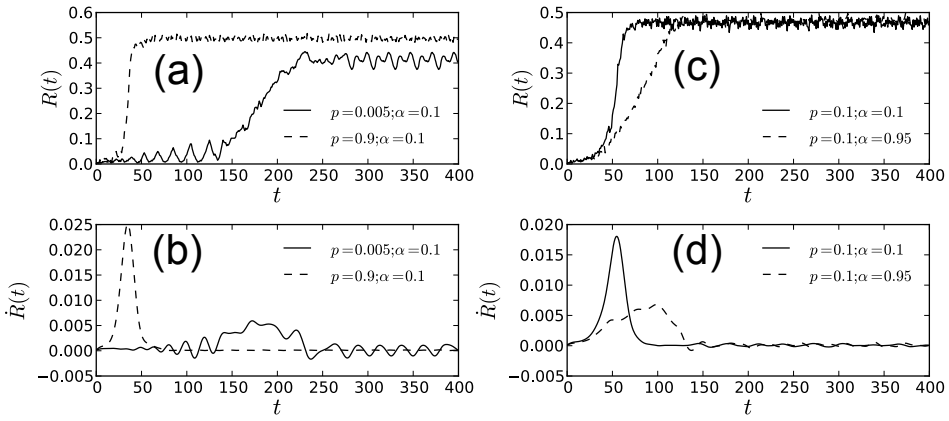

Fig. 5. Comparison of the evolution of the spike rate and its derivative for different values of p and α. Graphs obtained for the GSW model with 400 nodes.

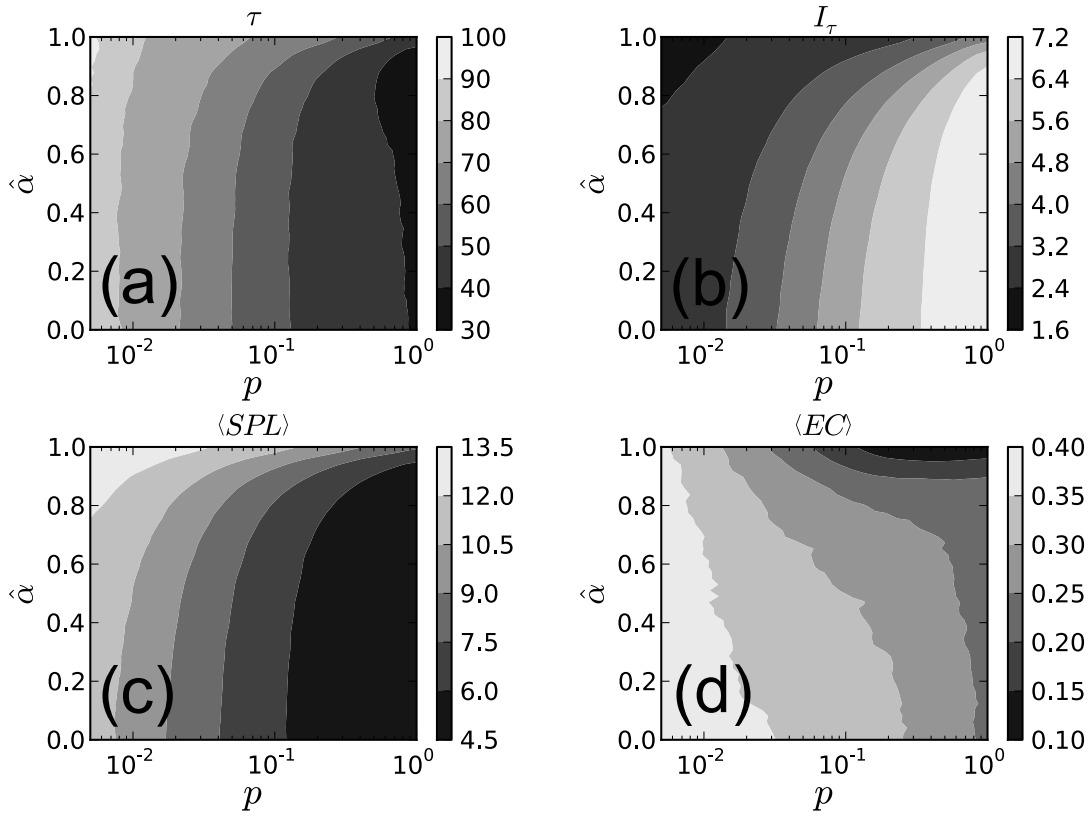

Fig. 6. Dynamical and structural measurements for the GSW model. (a) Time of the transition, τ, (b) intensity of the transition, I_τ, (c) average shortest path length between the source and the remaining nodes, and (d) the eigenvector centrality of the source.

6. Acknowledgments

References

Ahnert, S. E., Travençolo, B. A. N. & Costa, L. d. F. [2009] "Connectivity and dynamics of neuronal networks as defined by the shape of individual neurons," *New. J. Phys.* **11**, 103053.

Albert, R. & Barabási, A. L. [2002] "Statistical mechanics of complex network," *Rev. Mod. Phys.* **74**,

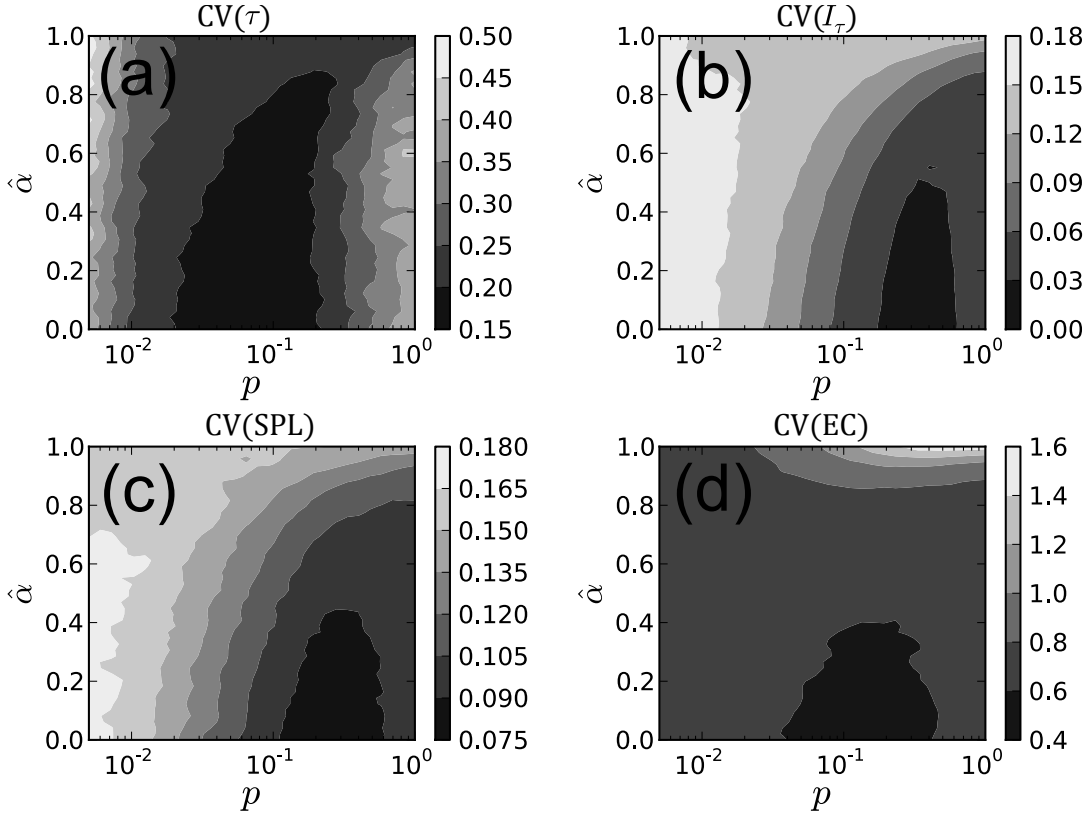

Fig. 7. Coefficient of variation (CV) of the measurements shown in Figure 6 for (a) Time of the transition, τ, (b) intensity of the transition, I_τ, (c) average shortest path length between the source and the remaining nodes, and (d) the eigenvector centrality of the source.

47–97.

Barrat, A., Barthelemy, M. & Vespignani, A. [2008] *Dynamical Process on Complex Networks* (Cambridge University Press).

Boccaletti, S., Latora, V., Moreno, Y., Chavez, M. & Hwang, D. U. [2006] "Complex networks: structure and dynamics," *Physics Reports* **424**, 175–308.

Costa, L. d. F., Rodrigues, F. A., Travieso, G. & Boas, P. R. V. [2007] "Characterization of complex networks: A survey of measurements," *Advances in Physics* **56**, 167–242.

D. Balcan, B. G. H. H. J. J. R. A. V., V. Colizza [2009] "Multiscale mobility networks and the spatial spreading of infectious diseases," *Proc Natl Acad Sci USA* **106**, 21484.

Dorogovtsev, S. N. & Goltsev, A. V. [2008] "Critical phenomena in complex networks," *Rev. Mod. Phys.* **80**, 1275–1335.

Erdős, P. & Rényi, A. [1960] "On the evolution of random graphs," *Publ. Math. Inst. Hung. Acad. Sci.* **5**, 17–61.

Gerstner, W. & Kistler, W. M. [2002] *Spiking Neuron Models* (Cambridge University Press).

Guardiola, X., Díaz-Guilera, A., Llas, M. & Pérez, C. J. [2000] "Synchronization, diversity, and topology of networks of integrate and fire oscillators," *Phys. Rev. E* **62**, 5565–5570.

Kinouchi, O. & Copelli, M. [2006] "Optimal dynamical range of excitable networks at criticality," *Nature Physics* **2**, 348–352.

Netoff, T. I., Clewley, R., Arno, S., Keck, T. & White, J. A. [2004] "Epilepsy in small-world networks," *The Journal of Neuroscience* **24(37)**, 8075–8083.

Newman, M. E. J. [2003] "The structure and function of complex networks," *SIAM Rev.* **45**, 167.

Newman, M. E. J. [2010] *Networks: An introduction* (Oxford University Press).

Rodrigues, F. A. & Costa, L. d. F. [2009] "Signal propagation in cortical networks: a digital signal processing

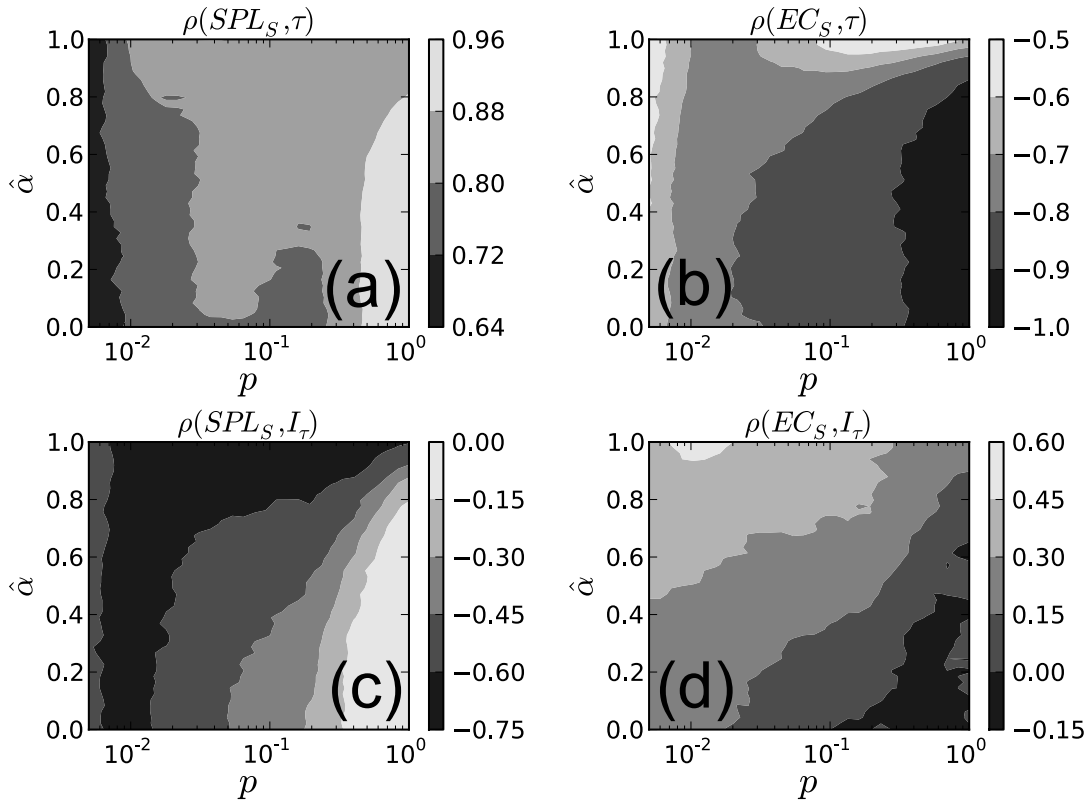

Fig. 8. Correlation between global structural and dynamical measurements. (a) $ASPL$ and τ, (b) EC and τ, (c) $ASPL$ and I_τ, and EC and I_τ. Results obtained after averaging over 1000 realizations of the GSW model with 400 nodes.

approach," *Frontiers in Neuroinformatics* **3(24)**, 1–13.

Rothkegel, A. & Lehnertz, K. [2009] "Multistability, local pattern formation, and global collective firing in a small-world network of nonleaky integrate-and-fire neurons," *Chaos* **19**, 015109.

Roxin, A., Riecke, H. & Solla, S. A. [2004] "Self-sustained activity in a small-world network of excitable neurons," *Phys. Rev. Lett.* **92 (19)**, 198101.

Sen, P., Banerjee, K. & Biswas, T. [2002] "Phase transitions in a network with a range-dependent connection probability," *Phys. Rev. E* **66**, 037102.

Watts, D. J. & Strogatz, S. H. [1998] "Collective dynamics of small-world networks," *Nature* **393**, 440–442.

Waxman, B. M. [1988] "Routing of multipoint connections," *IEEE J. Select. Areas. Commun.* **6**, 1617.

Wilson, H. R. & Cowan, J. D. [1972] "Excitatory and inhibitory interactions in localized populations of model neurons," *Biophysical Journal* **12**, 1–24.

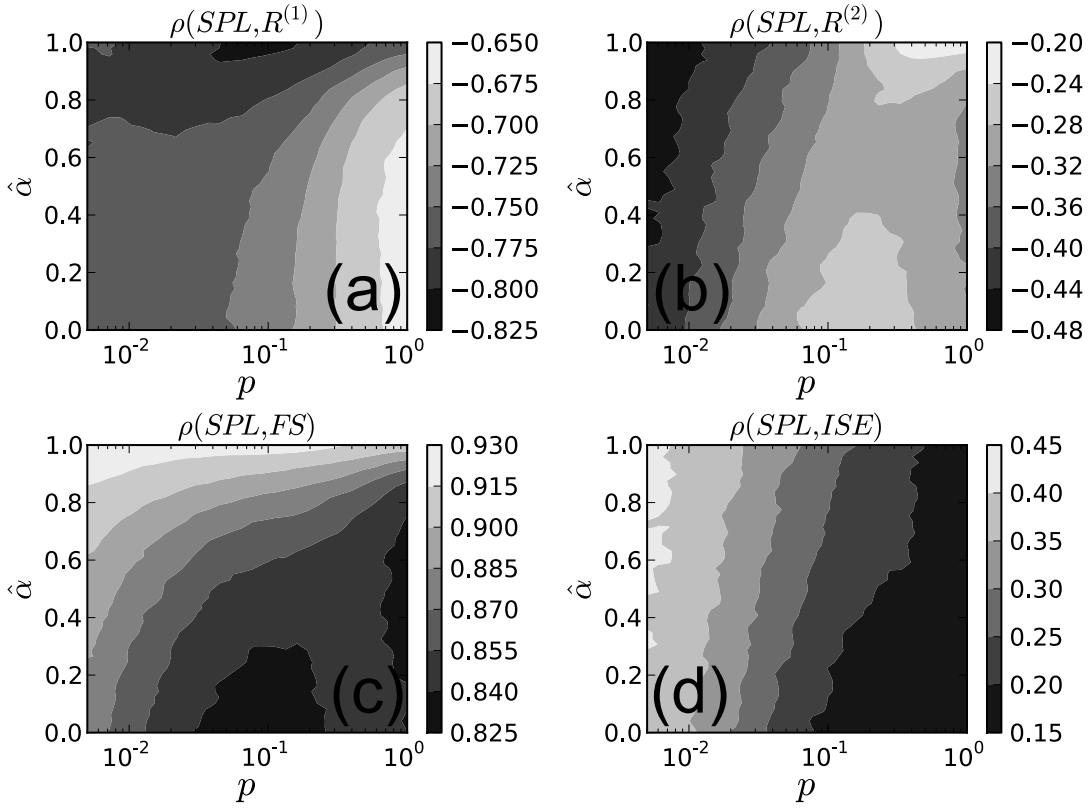

Fig. 9. Correlation between pairwise structural and dynamical measurements. (a) $ASPL$ and R_1, (b) EC and R_2, (c) $ASPL$ and FS, and EC and ISE. Results obtained after averaging over 1000 realizations of the GSW model with 400 nodes.